ACS Catalysis

RESEARCH ARTICLE

pubs.acs.org/acscatalysis

Facile Microwave-Refluxing Synthesis and Catalytic Properties of Vanadium Pentoxide Nanomaterials

Guohong Qiu,[†,‡] Saminda Dharmarathna,[‡] Homer Genuino,[‡] Yashan Zhang,[‡] Hui Huang,[‡] and Steven L. Suib*[,‡]

[†]Key Laboratory of Subtropical Agricultural Resources and Environment, Ministry of Agriculture, College of Resources and Environment, Huazhong Agricultural University, Wuhan, 430070, P.R. China

[‡]Department of Chemistry, University of Connecticut, 55 North Eagleville Road, Storrs, Connecticut, 06269-3060, United States

ABSTRACT:

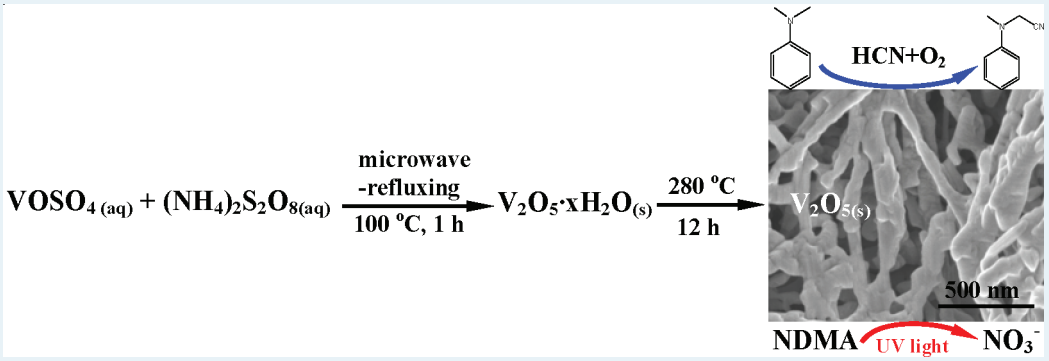

Vanadium pentoxide nanomaterials were prepared by a facile microwave-assisted refluxing reaction of $VOSO_4$ and $(NH_4)_2S_2O_8$ solutions under atmospheric pressure at 100 °C for 1 h. The synthesized products were characterized by X-ray diffraction, scanning electron microscopy, Fourier transform infrared spectroscopy, thermogravimetric analysis, and Brunauer−Emmett−Teller surface area measurements. The catalytic oxidation and photocatalytic activities of the synthesized V_2O_5 were evaluated by oxidative cyanation of *N*,*N*-dimethylaniline in methanol and photodegradation of *N*-nitrosodimethylamine (NDMA) in aqueous solution, respectively. $V_2O_5 \cdot xH_2O$ nanofibers were formed when $VOSO_4$ and $(NH_4)_2S_2O_8$ solutions were irradiated with microwaves under reflux conditions at 100 °C within 1 h. Nanostructured V_2O_5 was synthesized by calcining $V_2O_5 \cdot xH_2O$ at 280 °C for 12 h. The conversion of *N*,*N*-dimethylaniline to *N*-methyl-*N*-phenylcyanamide increased with an increase in the amount of V_2O_5 catalyst. As the amount of synthesized V_2O_5 increased from 10 to 15 mg, the conversion of *N*,*N*-dimethylaniline to *N*-methyl-*N*-phenylcyanamide reached 100%, but the selectivity decreased from 100% to 96%. *N*-methyl-*N*-phenylformamide was formed as a byproduct because of use of excess V_2O_5. The as-synthesized V_2O_5 nanomaterials showed comparable photocatalytic performance with commercial TiO_2 (P-25) for the degradation of *N*-nitrosodimethylamine to NO_3^- in water. This work provides a facile synthesis method of nanosized $V_2O_5 \cdot xH_2O$ and V_2O_5 with excellent catalytic activities.

KEYWORDS: vanadium pentoxide, microwave-refluxing, oxidative cyanation, photodegradation, *N*, *N*-dimethylaniline, *N*-nitrosodimethylamine

1. INTRODUCTION

In recent years, one-dimensional nanostructures have become the focus of intensive basic research because of their unique physicochemical properties and potential applications as nanoscale devices.[1] Among these, layered vanadium pentoxide (V_2O_5) nanomaterials have been extensively investigated for their prospective applications in chemical sensors, field emitters, electrochromic devices, and lithium-ion batteries,[2−6] particularly as effective catalysts.[7,8] Several efforts have been devoted to the fabrication of V_2O_5 nanomaterials with various morphologies. For example, hollow V_2O_5 nanoparticles were fabricated by laser ablation.[9] Thermal evaporation methods were also conducted to obtain V_2O_5 ultralong nanoribbons at 600−1050 °C.[10,11] V_2O_5 nanowires were hydrothermally synthesized at 120 °C for 24 h.[6] V_2O_5 hollow microspheres were obtained by hydrothermal reaction in organic solution followed by calcination at 500 °C for 2 h.[12] Centimeter long V_2O_5 nanowires were made by hydrothermal reaction at 205 °C for 4 d followed by calcination at 400 °C.[2] V_2O_5 nanoflowers were prepared by a multistep reaction of organic reagent and vanadium complex at room temperature for 24 h.[13] Thin films of $V_2O_5 \cdot nH_2O$ nanotube arrays and dendrites could be electrodeposited.[5,14] Single-crystal

Received: August 23, 2011
Revised: October 28, 2011
Published: November 02, 2011

V_2O_5 nanorod arrays were fabricated using electrochemical deposition in $VOSO_4$ aqueous solution with subsequent sintering at 485 °C.[15] However, as for conventional methods, high temperature, high pressure, and relatively long times are required for the preparation of V_2O_5. In contrast, unconventional methods based on chemical synthesis could provide an alternative and intriguing strategy for generating one-dimensional nanostructures in terms of material diversity, cost, throughput, and the potential for high-volume production.[1]

Microwave-assisted chemistry is based on the interaction between electric dipoles in dielectric materials, liquids, or solid materials and the applied electromagnetic field.[16] The growing interest in novel microwave processing can be attributed to several attractive features. Significant reduction in reaction time and energy costs are attributed to shorter processing times, rapid heating, and formation of homogeneous products.[16−18] Moreover, refluxing reactions under atmospheric pressure work at relatively low temperatures with simpler operations, higher productivity, lower cost, and can be easily controlled whenever necessary.[19] Therefore, microwave-assisted refluxing reactions have advantages of both microwave irradiation and refluxing reactions in materials synthesis and applications. This method significantly reduces the preparation time from days to minutes, and easily screens a wide range of experimental conditions to optimize and scale-up syntheses with low energy consumption. Anhydrous and hydrated V_2O_5 nanomaterials may also be prepared using microwave-assisted refluxing reaction techniques.

Vanadium pentoxide has been used as an effective catalyst for the oxidative cyanation of tertiary amines with molecular oxygen in the presence of sodium cyanide, acetic acid, which can substitute for noble-metal-containing catalysts, such as ruthenium trichloride, $[RuCl_2(PPh_3)_3]$ and $Pr_4N[RuO_4]$, because of their expensive nature and moisture sensitivity.[7,20,21] The conversions were compared for the oxidative cyanation of various tertiary amines with sodium cyanide by using V_2O_5 catalyst in a recent communication.[7] However, the influence of the amount of catalyst on product composition, as a byproduct in reaction system, and reaction process need to be further studied to scale-up the process.

N-nitrosodimethylamine (NDMA) can be released from agriculture, dye, cosmetic, and food processing, and naturally formed in the environment as a result of various chemical and biological processes.[22] Wastewater industries largely contribute to the presence of NDMA in the environment.[22] Removal of NDMA as a contaminant in the environment is still a challenge.[22−24] Surface fluorination techniques, changing crystal substructures, and doping methods were used to enhance the catalytic performance of TiO_2 and manganese oxides for the photodegradation of NDMA.[22,23] This method is an expeditious way to remove NDMA by photocatalytic degradation, and highly efficient photocatalysts should be chosen. Vanadium pentoxide catalysts are known to have excellent photocatalytic activities for the degradation of aniline, acetone, and rhodamine B in a wide range of wavelengths.[25−27] V_2O_5 synthesized by this facile method might also have some potential applications in the photocatalytic degradation of NDMA.

In this work, $V_2O_5 \cdot xH_2O$ nanobelts were synthesized by a microwave-assisted refluxing reaction at mild conditions within a short time. V_2O_5 nanomaterials were obtained after heat treatment of $V_2O_5 \cdot xH_2O$ at 280 °C for 12 h. The crystal structures, thermochemical behavior, specific surface areas, and morphologies of the as-prepared samples were characterized by X-ray diffraction (XRD), Fourier transform infrared spectroscopy (FTIR), thermogravimetric analysis (TGA), scanning electron microscopy (SEM), and Brunauer−Emmett−Teller (BET) surface area measurements. The catalytic oxidation and photocatalytic activities were evaluated by oxidative cyanation of *N*,*N*-dimethylaniline in methanol and photodegradation of *N*-Nitrosodimethylamine (NDMA) to NO_3^- in water, respectively.

2. EXPERIMENTAL SECTION

2.1. Materials and Chemicals. $(NH_4)_2S_2O_8 \cdot H_2O$ (≥98%), vanadium(IV) oxide sulfate hydrate (97%, vanadium content: 22%), NaCN (≥99%), Na_2SO_4 (≥99%), KNO_3 (≥99%), TiO_2 (Degussa P-25), V_2O_5 (99.6%), *N*,*N*-dimethylaniline (≥99%), and *N*-nitrosodimethylamine (NDMA) solution (≥99%, 200 mg L^{-1}) were all purchased from Sigma-Aldrich. Methanol (100%), acetic acid (99.9%), NaCl (≥99%), and $NaHCO_3$ (99%) were supplied by J. T. Baker. All reagents used were of analytical grade, unless otherwise noted.

2.2. Synthesis and Characterization of V_2O_5. A 2.695 g portion of $VOSO_4 \cdot nH_2O$ and 1.438 g of $(NH_4)_2S_2O_8 \cdot H_2O$ were mixed and dissolved into 100 mL of distilled deionized water (DDW) in a 250 mL round-bottomed flask, which was placed in a multimode CEM MARS 5 Microwave Chamber fitted with a reflux condenser and a Teflon coated magnetic stirrer. A fiber-optic temperature-measuring probe was directly inserted into the reaction mixture by using a Sapphire thermowell. The microwave-refluxing setup was illustrated in our previous report.[16] The microwave power was set to 300 W but fluctuated to maintain the input temperature value of 100 ± 2 °C with a ramp rate of 20 °C·min^{-1} and a holding time of 60 min. The resulting yellow precipitate was filtered and washed thoroughly with anhydrous ethanol and DDW several times. Finally, the as-obtained yellow powder product was dried in an oven at 60 °C for 12 h, and then calcined in air at a fixed temperature for 12 h.

The crystal structures of synthesized products were identified by XRD at room temperature using a Scintag XDS 2000 instrument with Cu Kα radiation. The diffractometer was operated at a tube voltage of 45 kV and a tube current of 40 mA. FTIR (Nicolet 8700) analysis was carried out on a Bruker Equinox 55 model spectrophotometer by making pellets with KBr powder, and the resolution was set at 4 cm^{-1} with a scan number of 32. Scanning electron microscopy (SEM) and energy-dispersive X-ray spectroscopy (EDX) were performed on the Zeiss DSM 982 Gemini field-emission gun SEM system. High-resolution transmission electron microscopy (HR-TEM) experiments were performed using a JEOL 2010 instrument with an accelerating voltage of 200 kV. The synthesized product was dispersed in ethanol, and a drop of the homogeneous dispersion was loaded on a carbon coated copper grid and allowed to dry before analysis.

The thermal stability of the samples was determined using an SDT Q600 thermogravimetric analyzer, and the sample was heated at a ramp rate of 1 °C min^{-1} in air. For BET analysis, about 0.2 g of powder sample was weighed and degassed at 120 °C for 12 h, and then the BET surface area of V_2O_5 was tested with a Quantachrome Autosorb-1-C automated N_2 gas adsorption system. Five point BET measurements were performed.

2.3. Catalytic Activity for Oxidative Cyanation of Tertiary Amines. The oxidative cyanation reactions of *N*,*N*-dimethylaniline were carried out in a batch reactor, following previous work.[7] Briefly, a 50 mL round-bottom flask with a magnetic stirrer, equipped with a reflux condenser and an oxygen balloon, was charged with *N*,*N*-dimethylaniline (1 mmol), methanol (1 mL), NaCN (1.2 mmol), and a measured quantity of the as-obtained

dx.doi.org/10.1021/cs200437x |*ACS Catal.* 2011, 1, 1702–1709

V_2O_5 or the same amount of commercially available V_2O_5. After the addition of acetic acid (0.3 mL) to the above system, the resulting mixture was continuously stirred under an oxygen or nitrogen atmosphere at 70 °C, which was controlled in a paraffin oil bath. After 1.5 h of reaction, the flask was lifted up above the oil level, and the reaction solution was allowed to cool down to room temperature. The aqueous $NaHCO_3$ was then added to the reaction mixture and extracted with ethyl acetate (3 × 10 mL). The combined organic layer was washed with brine, and dried over anhydrous sodium sulfate. The catalyst was recovered by filtration. Gas chromatography−mass spectrometry (GC-MS) was used to identify and quantify the products. GC-MS analyses were done on an HP 5890 series II chromatograph with a thermal conductivity detector coupled with an HP 5970 mass selective detector. An HP-1 column (nonpolar cross-linked siloxane) with dimensions of 12.5 m × 0.2 mm ×0.33 mm was used for separation.

2.4. Photocatalytic Activity for NDMA Degradation. In a typical experiment, 100 mg of V_2O_5 catalyst was added to a beaker containing 300 mL of 100 μM NDMA solution buffered with 4 mM bicarbonate and adjusted to pH 7.0 ± 0.1 by acid dilution using H_2SO_4. The heterogeneous mixture was then stirred for 30 min to attain equilibrium and sonicated for 15 min to uniformly disperse the catalyst particles prior to UV irradiation. For comparison purposes, experiments using commercial TiO_2 (Degussa P-25) (100 mg in 300 mL of 100 μM NDMA solution) and blank (without added catalyst) were also performed.

Sixteen UV lamps emitting mainly monochromatic light of λ = 254 nm installed on a *Rayonet* photochemical chamber reactor (Model RPR-200, Southern New England Ultraviolet Co. Inc.) were used as the constant source of UV light. The prepared mixture was transferred to a quartz beaker, covered, and positioned at the center of the photoreactor. UV photolysis times were at 10 min intervals from 0 to 60 min performed with continuous stirring of the mixture with 200 rpm at room temperature. A desired volume (~20 mL) was collected for each time interval. Suspended catalysts were recovered by centrifugation of the mixture for 10 min at 8000 rpm, and subsequent filtration through a Millipore filter with pore size of 0.45 μm.

Because of low percent recovery of NDMA in water during liquid−liquid extraction, NDMA was not systematically quantified. However, qualitative determination of the degradation of NDMA and the formed organic photoproducts were conducted using Direct Analysis in Real-Time Mass Spectrometer (DART-MS) AccuTOF-DART. Nitrate ions were measured using a UV spectrophotometric screening method (Standard Method 4500-NO_3^- B).[28] Nitrate standard solutions were prepared from KNO_3. All solutions were prepared using NDMA-free and nitrate-free ultrapure water (18 MΩ-cm).

3. RESULTS AND DISCUSSION

3.1. Preparation and Characterization of Vanadium Pentoxide. Figure 1a shows the XRD patterns of product fabricated by microwave-assisted refluxing reaction of $VOSO_4 \cdot nH_2O$ and $(NH_4)_2S_2O_8 \cdot H_2O$ solution at 100 °C for 1 h. Peaks with *d* spacings of 1.09, 0.37, 0.34, 0.26, 0.19, 0.18, and 0.13 nm, suggest that layered $V_2O_5 \cdot xH_2O$ was formed.[3,5,29,30] As for $V_2O_5 \cdot xH_2O$, the interlayer spacing *d* can be calculated from the diffraction angle of the (001) peak.[5] In the present work, the sample was treated at 60 °C for 12 h, and the interlayer spacing was observed as 1.09 nm (Figure 1a). When treated at 240 °C for 12 h, the *d* spacing of the (001) peak showed a slight decrease from 1.09 to 1.05 nm (Figure 1b), and this trend was consistent with previous results, possibly because of tightly bound water not being completely removed below 250 °C.[5] As the heat-treatment temperature increased to 280 °C, orthorhombic V_2O_5 (JCPDS card No. 41-1426) was formed (Figure 1c).

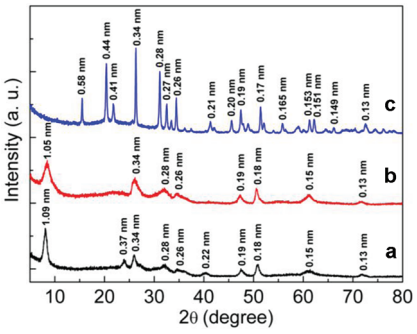

Figure 1. XRD patterns of the synthesized products with different heat treatment temperatures in air for 12 h: (a) 60 °C; (b) 240 °C; (c) 280 °C.

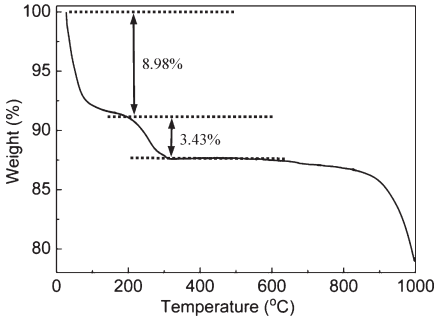

Figure 2. TGA curve of the synthesized $V_2O_5 \cdot xH_2O$.

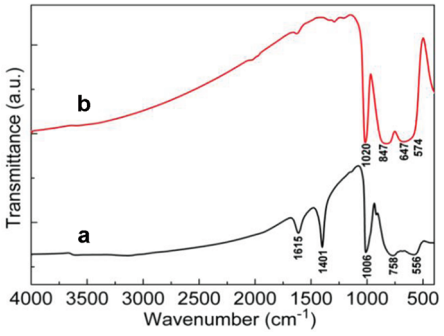

Figure 3. FTIR spectra of the synthesized products with different heat-treatment temperatures in air for 12 h: (a) 60 °C; (b) 280 °C.

The thermal dehydration process of hydrous vanadium pentoxide ($V_2O_5 \cdot xH_2O$) was further measured by thermogravimetric analysis as shown in Figure 2. The profile indicated the corresponding weight losses of H_2O and O_2 in a range from room temperature to 1000 °C, which were divided into three steps. The weight loss of 8.98% below 200 °C was likely attributed to physisorbed and chemisorbed water,[27] because the sample was only dried in an oven at 60 °C for 12 h. The weight loss of 3.43% in the 200−600 °C range was due to the

dx.doi.org/10.1021/cs200437x |ACS Catal. 2011, 1, 1702–1709

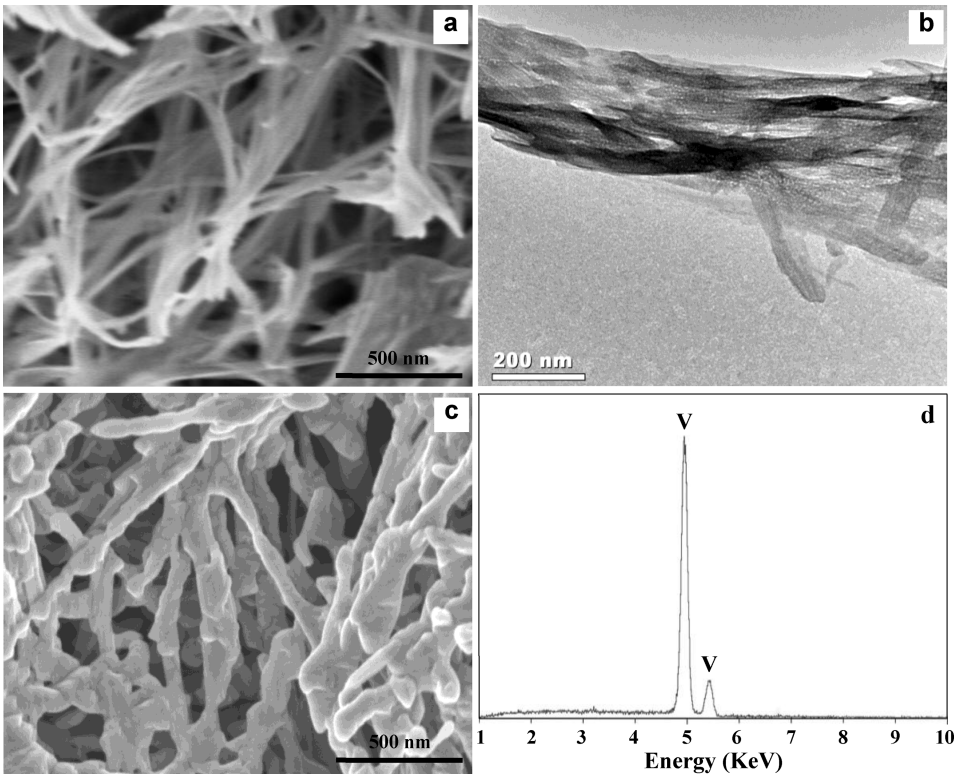

Figure 4. SEM and TEM images of the synthesized $V_2O_5 \cdot xH_2O$ (a, b), and SEM image and EDX spectrum of V_2O_5 (c, d).

release of chemically bonded water.[5,27] When temperature increased beyond 600 °C, the weight loss was assigned to the thermal decomposition of V_2O_5 with oxygen evolution.[9] Based on the TGA analysis and XRD patterns, the composition of the as-prepared hydrated vanadium pentoxide was suggested to be $V_2O_5 \cdot 0.4H_2O$. The values of interlayer spacing d for the (001) peak were 1.115 and 0.843 nm for $V_2O_5 \cdot 0.6H_2O$ and $V_2O_5 \cdot 0.3H_2O$, respectively.[5] In this work, the interlayer spacing d was found to be 1.09 nm for $V_2O_5 \cdot 0.4H_2O$. As reported, hydrated vanadium pentoxide could be dehydrated to V_2O_5 at near 300 °C according to the TGA curve.[5] The similar TGA curve was obtained, and weight loss tended toward stability in the range of 320 to 600 °C (Figure 2). A temperature of 280 °C was chosen to remove the chemically bonded water in the case of agglomeration of particles at higher temperatures.

To further confirm the structure of synthesized samples, the FTIR spectra of the $V_2O_5 \cdot xH_2O$ and V_2O_5 are shown in Figure 3. In the FTIR spectrum of $V_2O_5 \cdot xH_2O$, two peaks at 556 and 758 cm^{-1} (Figure.3a) were assigned to the V−O−V bending vibration and V−O−V asymmetric stretch, respectively.[29,31] The absorption peak at 1006 cm^{-1} was attributed to the stretching vibration of V═O.[31] The absorption band at 1401 cm^{-1} was due to hydrated vanadium oxides.[29,32] The peak at 1615 cm^{-1} was due to bending vibrations of water molecules,[6,29,31] and this peak had a hypsochromic shift of about 17 cm^{-1} in this experiment, which was probably due to the influence of vanadium−oxygen bonds in the structure. After heat-treatment at 280 °C for 12 h, the FTIR spectra were found to change remarkably because $V_2O_5 \cdot xH_2O$ was transformed into V_2O_5. Several peaks disappeared, and new peaks at 574, 647, 847, and 1020 cm^{-1} occurred. Peaks at 574 and 647 cm^{-1} were due to symmetric stretching vibrations of V−O−V.[31,33] Absorption bands at 847 and 1020 cm^{-1} were assigned to the asymmetric stretching vibration of V−O−V and stretching vibration of V═O, respectively. The absorption peak of water disappeared after heat treatment. The absorption peak of the stretching vibration of V═O shifted from 1006 to 1020 cm^{-1} after heat treatment likely due to the elimination of the influence of hydroxyl bonds on the stretching vibration of V═O. This similar trend was also observed in previous work.[34,35]

The morphologies of $V_2O_5 \cdot xH_2O$ and V_2O_5 were further characterized by SEM and TEM. As shown in Figure 4a, bunches of $V_2O_5 \cdot xH_2O$ nanobelts were formed from the microwave-assisted refluxing reaction of $VOSO_4$ and $(NH_4)_2S_2O_8$ solutions at 100 °C for 1 h. The $V_2O_5 \cdot xH_2O$ nanobelts of high flexibility twisted together in one bunch with a length greater than 1.0 μm (Figure 4b). After annealing in air at 280 °C for 12 h, V_2O_5 nanorods were formed, and coarsening of the nanobelts by sintering was observed (Figure 4c). The specific surface area of V_2O_5 was 16.6 $m^2\ g^{-1}$ likely due to the slight sintering and aggregation of nanorods. EDX analyses revealed that there was no impurity in the synthesized samples (Figure 4d), suggesting that the repeated filtration with distilled water several times and calcination could remove adsorbed anions on the surface of $V_2O_5 \cdot xH_2O$.

$V_2O_5 \cdot xH_2O$ is also an important catalyst in photochemistry and electrode materials for chemical power sources.[5,27] Various conventional methods have been reported to prepare $V_2O_5 \cdot xH_2O$.[3,5,27,29,30] $V_2O_5 \cdot xH_2O$ nanotubes were prepared via template-based physical wetting of V_2O_5 sol with two steps,[3] and a H_2O_2−V_2O_5 route has also been conducted to prepare $V_2O_5 \cdot xH_2O$.[5] However, these methods are multistep and V_2O_5 needs to be fabricated first. Hydrothermal reactions were performed to synthesize $V_2O_5 \cdot 0.9H_2O$ and $V_2O_5 \cdot 0.6H_2O$ nanomaterials.[27,29,30]

dx.doi.org/10.1021/cs200437x |ACS Catal. 2011, 1, 1702–1709

Table 1. V_2O_5-Catalyzed Oxidative Cyanation of *N,N*-Dimethylaniline with Sodium Cyanide[a]

catalyst mass (mg)	atmosphere	conversion (%)	selectivity (%)
0	O_2	3	100
5	O_2	66	100
10	O_2	80	100
15	O_2	100	96
15	N_2	0	NA

[a] Reaction condition: *N,N*-dimethylaniline (1 mmol), NaCN (1.2 mmol), MeOH (1 mL), AcOH (0.3 mL), at 70 °C for 1.5 h. Conversions determined by GC-MS. NA: Not applicable.

Scheme 1. Reaction Equation for the Oxidative Cyanation of *N,N*-Dimethylaniline

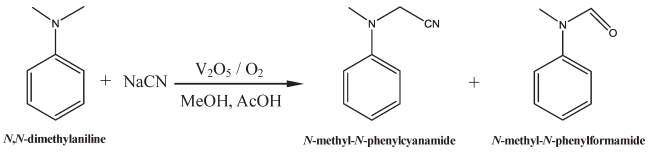

However, high temperature, high pressure, and relatively long times are required. In the present work, $V_2O_5 \cdot xH_2O$ nanobelts were rapidly synthesized with one step and low energy cost. The lowest temperature for the transformation of $V_2O_5 \cdot xH_2O$ to V_2O_5 was also studied. Nanosized V_2O_5 rods could be obtained by the calcination of $V_2O_5 \cdot xH_2O$ at 280 °C, and their morphologies were nearly uniform although slight sintering and aggregation occurred.

3.2. Catalytic Oxidation Performance for Cyanation of Tertiary Amines. Catalytic oxidative cyanation of *N,N*-dimethylaniline in methanol was studied, and the influence of dosage of the synthesized V_2O_5 catalyst on the conversion and selectivity of *N,N*-dimethylaniline to *N*-methyl-*N*-phenylcyanamide was conducted using molecular oxygen as oxidant at 70 °C for 1.5 h. The as-synthesized V_2O_5 materials exhibited excellent catalytic oxidative cyanation activities, and the conversions are shown in Table 1. The conversion of *N,N*-dimethylaniline to *N*-methyl-*N*-phenylcyanamide was only about 3% without adding V_2O_5 catalyst. As the amount of catalyst V_2O_5 increased to 5.0 and 10.0 mg, the conversion was raised to 66% and 80%, respectively. When the used V_2O_5 was no more than 10 mg in the above reactions, *N*-methyl-*N*-phenylcyanamide was formed with a selectivity of 100%. The conversion was increased with an increase in the amount of catalyst, likely due to more oxygen molecules being adsorbed onto V_2O_5, and then more oxidation active sites could be provided. When 15 mg of V_2O_5 was used, the conversion reached 100%. However, the selectivity decreased to 96%, and byproduct *N*-methyl-*N*-phenylformamide was formed with a yield of 4%. Scheme 1 gives the equation for the oxidative cyanation of *N,N*-dimethylaniline based on the compositions of the products.

The conversion of *N,N*-dimethylaniline to *N*-methyl-*N*-phenylcyanamide was 99% when 9.2 mg of V_2O_5 (5 mol %) catalyst was performed at 60 °C.[7] However, the conversion was only 80% when 10 mg of V_2O_5 catalyst was conducted at 70 °C, and increased to 100% as 15 mg of catalyst was used instead in this work. The difference in the catalytic efficiency was likely due to (*i*) different specific surface areas of V_2O_5 catalysts. In this work, the specific surface area of the synthesized V_2O_5 nanorods was

Scheme 2. Proposed Reaction Mechanism for the V_2O_5-Catalyzed Oxidative Cyanation of *N,N*-Dimethylaniline

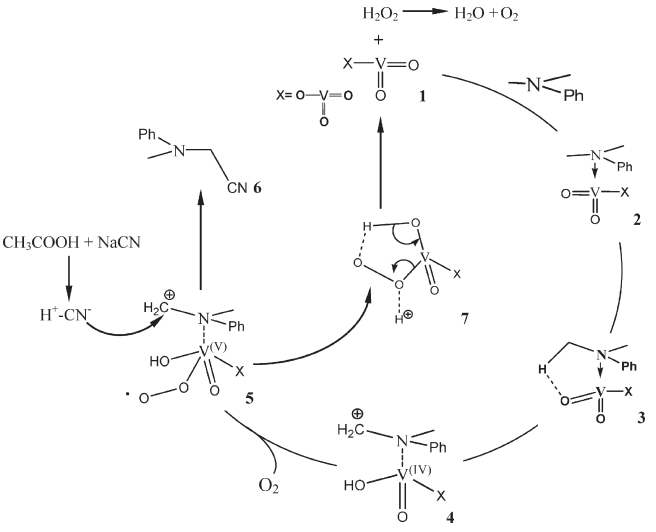

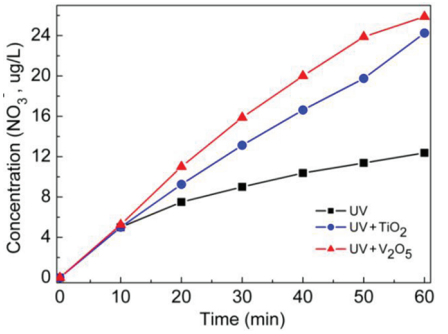

Figure 5. Concentration of NO_3^- during the photodegradation of NDMA (100 μM, 300 mL) with different catalysts (100 mg).

16.6 $m^2\ g^{-1}$ likely due to slight sintering and aggregation during the calcination process. The preparation method, SEM morphology, and BET surface area measurements were not reported in the communication.[7] The specific surface area might be larger in the reported work and contributed to the higher efficiency. (*ii*) Different sample pretreatment methods. This catalytic reaction was sensitive to moisture and water; however, V_2O_5 is usually contaminated by water after storage or operation in air. The commercial V_2O_5 sample of 10 mg was also studied in this catalytic reaction, and the conversion and selectivity for the oxidative cyanation of *N,N*-dimethylaniline were 69% and 98%, respectively. In this work, the as-prepared V_2O_5 showed better catalytic performance than commercial V_2O_5 under the same reaction conditions. The BET specific surface area of the purchased V_2O_5 was characterized to be 3.0 $m^2\ g^{-1}$, and the surface area of the as-obtained V_2O_5 was 16.6 $m^2\ g^{-1}$. These results further showed that specific surface area possibly affects the catalytic performance. The catalytic experiment should be further performed with proper sample pretreatment methods in dry environments.

A definite reaction mechanism for the above equation has not been established because of the difficulties in determining intermediates, and the reaction may proceed through a radical mechanism.[7] Compared with similar experimental condtions and

dx.doi.org/10.1021/cs200437x |*ACS Catal.* 2011, 1, 1702–1709

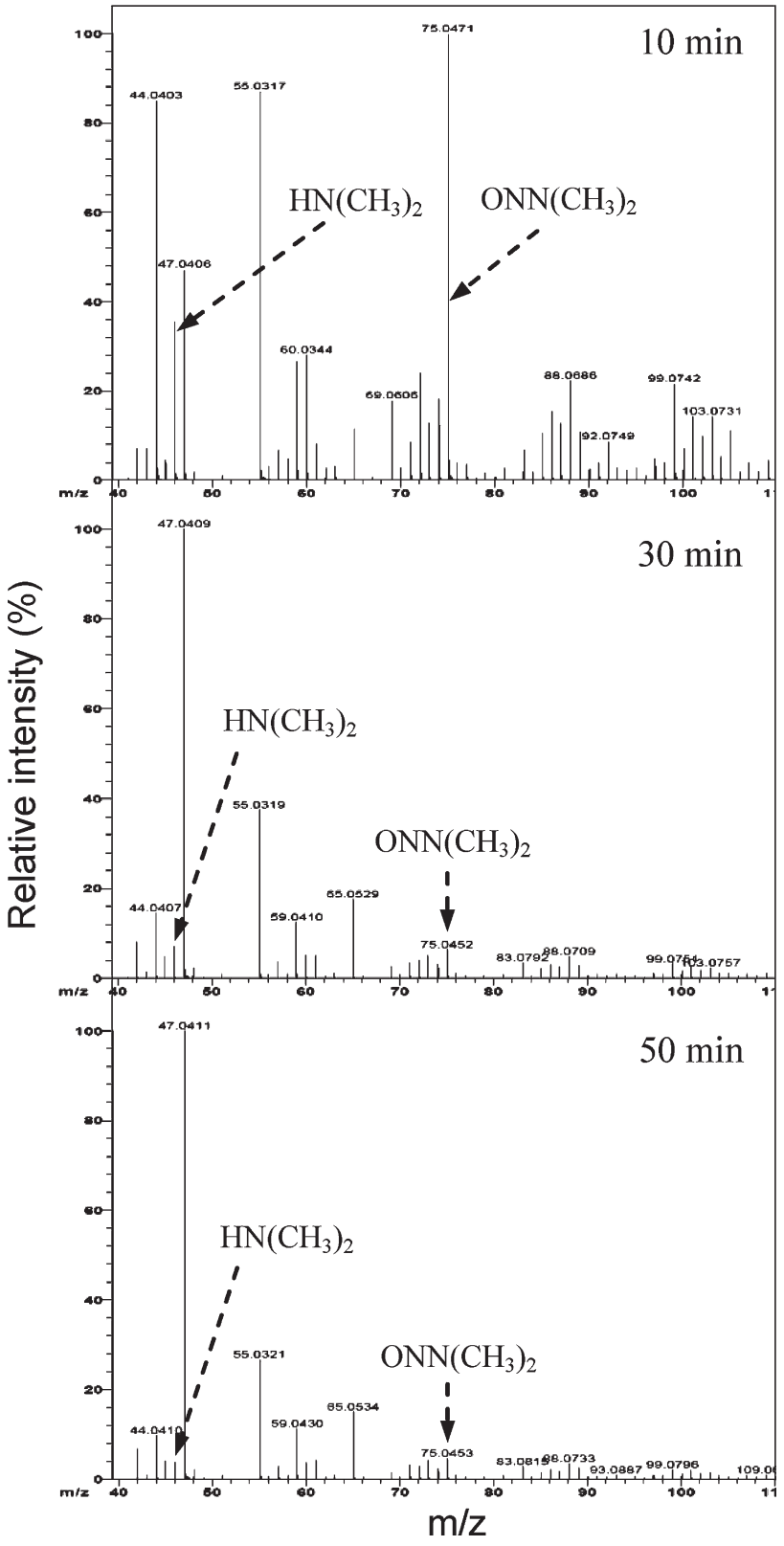

Figure 6. ESI mass spectra for monitoring the photodegradation of NDMA by the synthesized V_2O_5 over 50 min.

products,[7,20,21] the reaction mechanism for a plausible pathway in the present work is suggested in Scheme 2.

As proposed in Scheme 2, Lewis acid sites on V_2O_5 accepted a lone pair of electrons on nitrogen in *N*,*N*-dimethylaniline to form intermediate **2** for the coordination between the tertiary amine and the vanadium pentoxide. A hydrogen bond was formed between the hydrogen atom on α-carbon and oxygen on vanadium oxide, giving rise to intermediate **3** having a five membered ring.

dx.doi.org/10.1021/cs200437x |*ACS Catal.* 2011, 1, 1702–1709

Subsequently, intermediate **4** was formed via α-hydrogen transfer from the α-carbon to an oxygen atom on vanadium oxide.[7] Oxidation of intermediate **4** with molecular oxgyen led to the formation of vanadium(V) superoxo intermediate **5**, where nucleophilic attack occurred by CN^- in HCN (generated in situ from NaCN and acetic acid) to yield *N*-methyl-*N*-phenylcyanamide (Product **6**) and regenerate V_2O_5, and intermediate **7** was likely to be produced in this process.

As the proposed mechanism, oxygen participated in the reaction and played a very important role as oxidant. To confirm that V_2O_5 and O_2 functioned as the catalyst and oxidant, respectively, catalytic oxidative cyanation reaction was carried out under nitrogen. No target product was formed. Combined with the result of conversion of 3% without adding V_2O_5 in oxygen atmosphere (Table 1), O_2 acts as an oxidant for the oxidative cyanation of *N*,*N*-dimethylaniline to *N*-methyl-*N*-phenylcyanamide, and V_2O_5 can clearly catalyze the conversion.

In this work, only when the used catalyst V_2O_5 was excessive, was *N*-methyl-*N*-phenylformamide produced and affected the selectivity of the target product in the oxidative cyanation process. This is likely due to three possibilities. (*i*) The competitive reaction of methanol and sodium cyanide and rearrangement in the oxidation process of *N*,*N*-dimethylaniline. Possibly because of the stronger Lewis basicity of CN^-, oxidative cyanation occurred first, and methanol participated in the reaction only when the catalyst was excessive. (*ii*) The transformation of intermediate **5** is likely due to affinity and rearrangement of α-carbon positive ions and peroxygen and radicals. (*iii*) The further oxidation of *N*-methyl-*N*-phenylcyanamide (Product **6**). To examine the possibile reactions in the process, 1 mmol of *N*,*N*-dimethylaniline, 1 mL of methanol, 0.3 mL of acetic acid, and 15 mg of V_2O_5 were mixed and allowed to react at 70 °C under an oxygen atmosphere in the absence CN^-. *N*-methyl-*N*-phenylformamide was not detected, and the conversion of *N*,*N*-dimethylaniline was zero, suggesting that reaction (*i*) did not occur. To further prevent the in situ formation of CN^-, both acetic acid and sodium cyanide were eliminated from the above reaction; *N*-methyl-*N*-phenylformamide was also not formed, suggesting that processes (*i*) and (*ii*) did not happen. Therefore, the byproduct of *N*-methyl-*N*-phenylformamide was formed likely because of the further oxidation of *N*-methyl-*N*-phenylcyanamide and V_2O_5 catalyst participating in the reaction. Determination of possible intermediates and the reaction mechanism is currently underway.

Compared with the reported experiment about oxidative cyanation of tertiary amines,[7] the present work further investigated the influence of catalyst amount, starting materials on the reaction process, and conversion. These results revealed that V_2O_5 only worked as catalyst although it possesses high oxidation activity, and the byproduct of *N*-methyl-*N*-phenylformamide likely resulted from further oxidation of *N*-methyl-*N*-phenylcyanamide with the participation of V_2O_5. To improve the selectivity, proper reaction conditions need to be controlled.

3.3. Photocatalytic Activity for NDMA Degradation. In our previous and other reported work,[22,23] NDMA structure was destroyed at a fast rate forming photoproducts. The N−N bond in the photoexcited NDMA was cleaved forming ·NO fragments, which eventually formed the stable NO_3^-. NO_3^- was one of the major and stable oxidation products of NDMA;[22−24] therefore, the concentration of NO_3^- was one of the most important indices in evaluating the catalytic performance of TiO_2, Mn_3O_4, Pt-Mn_3O_4, and Pt-TiO_2.[23,24] In this work, the photocatalytic activity of V_2O_5 for NDMA degradation was investigated by monitoring the concentration of NO_3^-. Figure 5 shows the formation of NO_3^- as a function of UV irradiation time. The NO_3^- concentration increased with increasing irradiation time. In the absence of any catalyst, 12.4% of NDMA were converted to NO_3^- after 60 min of UV illumination. This was consistent with the results of our previous studies.[23] Using the catalysts alone under dark conditions did not produce NO_3^- ions in solution. When TiO_2 (P-25) was added to the solution system, and conversion of NDMA to NO_3^- was increased to 24.3%, whereas using V_2O_5 instead, a conversion of about 25.9% was obtained. The above results suggested that the as-obtained V_2O_5 catalyst has a comparable photocatalytic activity with TiO_2 (P-25).

Qualitative determination for NDMA was conducted using direct analysis in a real-time mass spectrometer, and part of the ESI-MS spectra are shown in Figure 6. The peak at m/z = 75.05 was attributed to the starting material of NDMA [$ONN(CH_3)_2$]. After 10 min of the photodegradation, a strong signal at m/z = 46.06 was observed, corresponding to the intermediate product DMA [$(CH_3)_2NH$], which was an important intermediate in the process.[22] The peak intensity of NDMA and DMA decreased remarkably when the photocatalytic reaction was conducted over 30 min (Figure 6), which further suggested that the as-prepared V_2O_5 was an excellent photocatalyst. Quantitative characterization for the degradation of NDMA in water should be conducted using continuous liquid−liquid extraction prior to gas chromatographic analysis in future studies.

4. CONCLUSIONS

$V_2O_5 \cdot xH_2O$ nanobelts have been prepared from $VOSO_4$ and $(NH_4)_2S_2O_8$ solutions by a microwave-assisted refluxing method for 1 h at 100 °C under atmospheric pressure. V_2O_5 nanowires could be fabricated after heat-treatment of $V_2O_5 \cdot xH_2O$ in air at 280 °C for 12 h. The as-obtained V_2O_5 showed excellent catalytic performance for the oxidative cyanation of *N*,*N*-dimethylaniline to *N*-methyl-*N*-phenylcyanamide. One mmol of *N*,*N*-dimethylaniline was completely transformed into *N*-methyl-*N*-phenylcyanamide with selectivity of 96% and *N*-methyl-*N*-phenylformamide (4%) when 15 mg of V_2O_5 was used at 70 °C for 1.5 h. For the photodegradation of NDMA to NO_3^-, the as-prepared V_2O_5 exhibited better catalytic performance than commercial TiO_2 (P-25). This route is of commercial interest as multigram quantities of $V_2O_5 \cdot xH_2O$ and V_2O_5 nanomaterials are produced rapidly under ambient pressure and could result in significant energy savings. The reaction mechanism of oxidative cyanation of *N*,*N*-dimethylaniline and quantitative determination for the degradation of NDMA will be studied in future work.

AUTHOR INFORMATION

Corresponding Author

*E-mail: Steven.Suib@uconn.edu. Phone: 1 860 486 2797. Fax: 1 860 486 2981.

Funding Sources

The authors thank the National Natural Science Foundation of China (Grants 41171375, 40830527, and 20807019) and the Fundamental Research Funds for the Central Universities (Program no. 2011PY015) for financial support. The authors acknowledge the U.S. Department of Energy, Office of Basic Energy Sciences, Division of Chemical, Geochemical and Biological Sciences for support of this work.

REFERENCES

(1) Xia, Y.; Yang, P.; Sun, Y.; Wu, Y.; Mayers, B.; Gates, B.; Ying, Y.; Kim, F.; Yan, H. *Adv. Mater.* **2003**, *15*, 353–389.

(2) Zhai, T.; Liu, H.; Li, H.; Fang, X.; Liao, M.; Li, L.; Zhou, H.; Koide, Y.; Bando, Y.; Golberg, D. *Adv. Mater.* **2010**, *22*, 2547–2552.

(3) Zhou, C.; Mai, L.; Liu, Y.; Qi, Y.; Dai, Y.; Chen, W. *J. Phys. Chem. C* **2007**, *111*, 8202–8205.

(4) Mai, L. Q.; Dong, Y. J.; Xu, L.; Han, C. H. *Nano Lett.* **2010**, *10*, 4273–4278.

(5) Wang, Y.; Cao, G. *Chem. Mater.* **2006**, *18*, 2787–2804.

(6) Xiong, C.; Aliev, A. E.; Gnade, B.; Balkus, K. J. *ACS Nano* **2008**, *2*, 293–301.

(7) Singhal, S.; Jain, S. L.; Sain, B. *Chem. Commun.* **2009**, 2371–2372.

(8) Routray, K.; Zhou, W.; Kiely, C. J.; Wachs, I. E. *ACS Catal.* **2011**, *1*, 54–66.

(9) Levi, R.; Bar-Sadan, M.; Albu-Yaron, A.; Popovitz-Biro, R.; Houben, L.; Shahar, C.; Enyashin, A.; Seifert, G.; Prior, Y.; Tenne, R. *J. Am. Chem. Soc.* **2010**, *132*, 11214–11222.

(10) Yan, B.; Liao, L.; You, Y.; Xu, X.; Zheng, Z.; Shen, Z.; Ma, J.; Tong, L.; Yu, T. *Adv. Mater.* **2009**, *21*, 2436–2440.

(11) Velazquez, J. M.; Banerjee, S. *Small* **2009**, *5*, 1025–1029.

(12) Cao, A. M.; Hu, J. S.; Liang, H. P.; Wan, L. J. *Angew. Chem., Int. Ed.* **2005**, *44*, 4391–4395.

(13) Parida, M. R.; Vijayan, C.; Rout, C. S.; Sandeep, C. S. S.; Philip, R.; Deshmukh, P. C. *J. Phys. Chem. C* **2011**, *115*, 112–117.

(14) Lee, J. K.; Kim, G. P.; Song, I. K.; Baeck, S. H. *Electrochem. Commun.* **2009**, *11*, 1571–1574.

(15) Takahashi, K.; Limmer, S. J.; Wang, Y.; Cao, G. Z. *J. Phys. Chem. B* **2004**, *108*, 9795–9800.

(16) Nyutu, E. K.; Chen, C. H.; Sithambaram, S.; Crisostomo, V. M. B.; Suib, S. L. *J. Phys. Chem. C* **2008**, *112*, 6786–6793.

(17) Opembe, N. N.; King'ondu, C. K.; Espinal, A. E.; Chen, C. H.; Nyutu, E. K.; Crisostomo, V. M.; Suib, S. L. *J. Phys. Chem. C* **2010**, *114*, 14417–14426.

(18) Qiu, G. H.; Huang, H.; Genuino, H.; Opembe, N.; Stafford, L.; Dharmarathna, S.; Suib, S. L. *J. Phys. Chem. C* **2011**, *115*, 19626–19631.

(19) Song, C. H.; Li, R. Q.; Liu, F.; Feng, X. H.; Tan, W. F.; Qiu, G. H. *Electrochim. Acta* **2010**, *55*, 9157–9165.

(20) Murahashi, S. I.; Komiya, N.; Terai, H.; Nakae, T. *J. Am. Chem. Soc.* **2003**, *125*, 15312–15313.

(21) Murahashi, S. I.; Komiya, N.; Terai, H. *Angew. Chem., Int. Ed.* **2005**, *44*, 6931–6933.

(22) Lee, J.; Choi, W.; Yoon, J. *Environ. Sci. Technol.* **2005**, *39*, 6800–6807.

(23) Genuino, H. C.; Njagi, E. C.; Benbow, E. M.; Hoag, G. E.; Collins, J. B.; Suib, S. L. *J. Photochem. Photobiol. A* **2011**, *217*, 284–292.

(24) Chaplin, B.; Schrader, G.; Farrell, J. *Environ. Sci. Technol.* **2010**, *44*, 4264–4269.

(25) Karunakaran, C.; Senthilvlan, S. *J. Colloid Interface Sci.* **2005**, *289*, 466–471.

(26) He, Y. M.; Wu, Y.; Sheng, T. L.; Wu, X. T. *Catal. Today* **2010**, *158*, 209–214.

(27) Li, B. X.; Xu, Y.; Rong, G. X.; Jing, M.; Xie, Y. *Nanotechnology* **2006**, *17*, 2560–2566.

(28) Eaton, A. D.; Clesceri, L. S.; Rice, E. W.; Greenberg, A. E. *Standard methods for the examination of water and wastewater*, 21st ed. (Centennial ed.); American Public Health Association, American Water Works Association, and Water Environment Federation: Washington, DC, 2005.

(29) Yang, Y.; Zhu, Q. Y.; Jin, A. P.; Chen, W. *Solid State Ionics* **2008**, *179*, 1250–1255.

(30) Li, G. C.; Pang, S. P.; Jiang, L.; Guo, Z. Y.; Zhang, Z. K. *J. Phys. Chem. B* **2006**, *110*, 9383–9386.

(31) Menezes, W. G.; Reis, D. M.; Benedetti, T. M.; Oliveira, M. M.; Soares, J. F.; Torresi, R. M.; Zarbin, A. J. G. *J. Colloid Interface Sci.* **2009**, *337*, 586–593.

(32) Yu, L.; Zhao, C. X.; Long, X.; Chen, W. *Microporous Mesoporous Mater.* **2009**, *126*, 58–64.

(33) Mohan, V. M.; Hu, B.; Qiu, W. L.; Chen, W. *J. Appl. Electrochem.* **2009**, *39*, 2001–2006.

(34) Epifani, M.; Andreu, T.; Magana, C. R.; Arbiol, J.; Siciliano, P.; D'Arienzo, M.; Scotti, R.; Morazzoni, F.; Morante, J. R. *Chem. Mater.* **2009**, *21*, 1618–1626.

(35) Ferreira, O. P.; Filho, A. G. S.; Alves, O. L. *J. Nanopart. Res.* **2010**, *12*, 367–372.